Supplement A: Below-cloud evaporation calculated by isotope

Stewart (1975) suggested the falling raindrop isotopic fractionation of evaporation could be calculated according to the fraction of raindrop mass remained after evaporation:

$$\Delta\delta=\delta_p-\delta_{zp\text{-}eq}=(1-\frac{\gamma}{\alpha})(F_{iso}^{\beta}-1) \quad \text{(eq1)}$$

where δ_p and $\delta_{zp\text{-}eq}$ are precipitation isotope ratio near the ground and below the cloud base, respectively; F_{iso} is the remaining fraction of raindrop mass after evaporation (hereafter, the remaining fraction of raindrop mass calculated by this method is denoted as F_{iso}); and the parameters of γ and β (Stewart, 1975) are defined as:

$$\gamma=\frac{\alpha h}{1-\alpha\left(D/D'\right)^{k}(1-h)} \quad \text{(eq2)}$$

$$\beta=\frac{1-\alpha\left(D/D'\right)^{k}(1-h)}{\alpha\left(D/D'\right)^{k}(1-h)} \quad \text{(eq3)}$$

where α are equilibrium fractionation factors for hydrogen and oxygen isotopes, respectively (Ellehoj et al., 2013; Horita and Wesolowski, 1994); h is relative humidity; D/D' for ^{2}H and ^{18}O are 1.024 and 1.0289, respectively (Stewart, 1975; Wang et al., 2016); and k is 0.58.

In turn, if the differences of isotopic composition during the falling raindrop evaporation and the parameters (e.g. γ, β, and α) are determined, the evaporated part of raindrop mass can be precisely calculated. The precipitation isotopic composition at the cloud base follows the equilibrium fractionation with the ambient water vapor, and is defined as:

$$R_{zp\text{-}eq}=R_{zv}\alpha \quad \text{(eq4)}$$

and can be equivalently rewritten in δ-notation as:

$$\frac{\delta_{zp\text{-}eq}}{1000}+1=\alpha\left(\frac{\delta_{zv}}{1000}+1\right) \quad \text{(eq5)}$$

and the water vapor isotopic composition at the cloud base follows the vertical distribution described by the following equation (Araguás-Araguás et al., 2000; Deshpande et al., 2010):

$$\delta_{zv}=1000\{\left(1+1000\delta_{gr\text{-}v}\right)\exp\left(-(\alpha-1)\left(Z/Z_0\right)\right)\}-1000 \quad \text{(eq 6)}$$

where α is the equilibrium fractionation factor at a temperature of the height of Z, and Z is the height of the cloud base, and Z_0 denotes scale height of atmospheric water vapor distribution. The values of Z_0 in low latitudes are discussed by Parameswaran and Krishnamurthy (1990). According to the mean moist adiabatic lapse rate, the cloud

base temperature can be expressed as:

$$T_z=6.5\times10^{-3}\ \mathrm{K/m} \qquad \text{(eq7)}$$

and here, the cloud base is assumed at about the 850 hPa (~1500 m) isobaric level.

Suppl. B: Below-cloud evaporation calculated by mass conservation model

Before the advent of the laser-based spectrometer, the method, which calculates the remaining fraction of raindrop mass according to the law of conservation of mass (hereafter, the remaining fraction of raindrop mass calculated by this method is denoted as $F_{raindrop}$), has been widely used (Kong et al., 2013; Li et al., 2016; Sun et al., 2020; Wang et al., 2016; Zhao et al., 2019):

$$F_{raindrop}=\frac{m_{end}}{m_{end}+m_{ev}} \qquad \text{(eq8)}$$

where the mass of the reaching ground raindrop without evaporation is m_{end} and the evaporated raindrop mass is m_{ev} which is defined as:

$$m_{ev}=Et \qquad \text{(eq9)}$$

where E denotes the evaporation intensity (the loss of water mass per unit time) and t stands for the falling time of a raindrop. The falling time of raindrop is assumed to be only related to the height of the cloud base, expressed as Z, and to the terminal velocity of a raindrop, expressed as v_{end}, and the equation can be defined as:

$$t=\frac{Z}{v_{end}} \qquad \text{(eq10)}$$

here the basic height of the cloud base is set as 1500m.

According to Best (1950a) the terminal velocity of the raindrop is considered by:

$$v_{end}=\begin{cases} 9.58e^{0.0354Z}\left(1-e^{-(D/1.77)^{1.147}}\right), & 0.3\le D<6.0 \\ 1.88e^{0.0256Z}\left(1-e^{-(D/0.304)^{1.819}}\right), & 0.05\le D<0.3 \\ 28.40D^2e^{0.0172Z}, & D<0.05 \end{cases} \qquad \text{(eq11)}$$

The evaporation intensity of falling drops is determined by a matrix which is composed of Q1 and Q2 (Kinzer and Gunn, 1951):

$$E=Q1(T,D)Q2(T,h) \qquad \text{(eq12)}$$

where Q1 is part of the function (cm) which is related to the ambient air temperature and raindrop diameter, and Q2 part (g cm^{-1} s^{-1}) is combination of air temperature and relative humidity. Following the results of Kinzer and Gunn (1951), the values of Q1 and Q2 for specific conditions are acquired by using a bilinear interpolation method which is suggested by Wang et al. (2016).

To estimate the raindrop diameter, an empirical formula suggested by Best (1950b) is applied:

$$1-F=e^{-(D/AI^q)^c} \quad \text{(eq13)}$$

where F is the fraction of raindrops with diameter less than D; I is precipitation intensity (mm h−1) which can be calculated according to the precipitation amount and duration; c, A, and q are constants of 2.25, 1.30, and 0.232, respectively. Assuming F = 0.5, the median size of the raindrop is solved as:

$$D_{50}=\sqrt[c]{0.69}AI^q \quad \text{(eq14)}$$

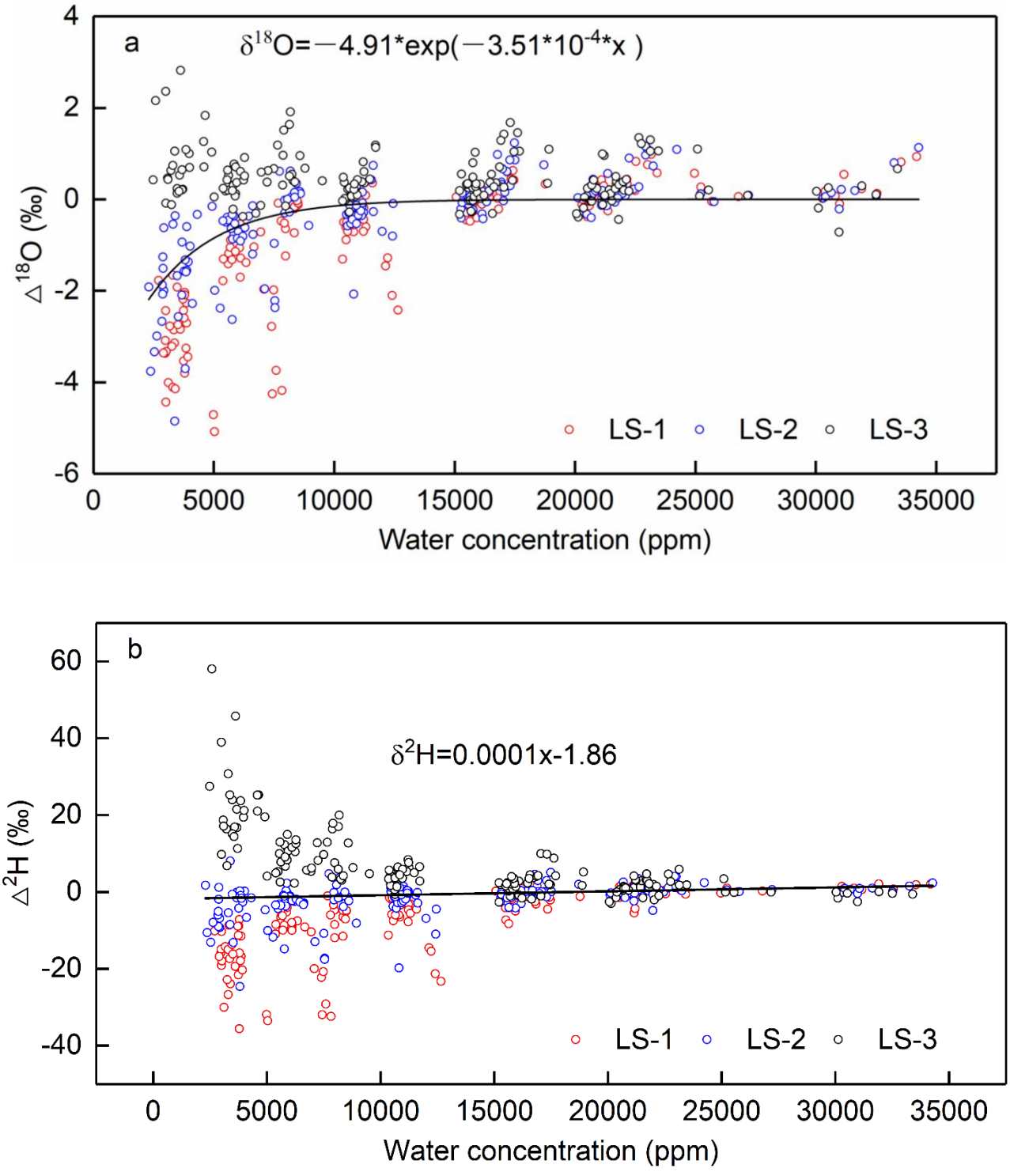

Figure S1 The humidity calibration for water vapor $\delta^{18}O_v$ (a); the same as (a), but for water vapor $\delta^{2}H_v$ (b); LS-1, LS-2, and LS-3 are three lab standards.

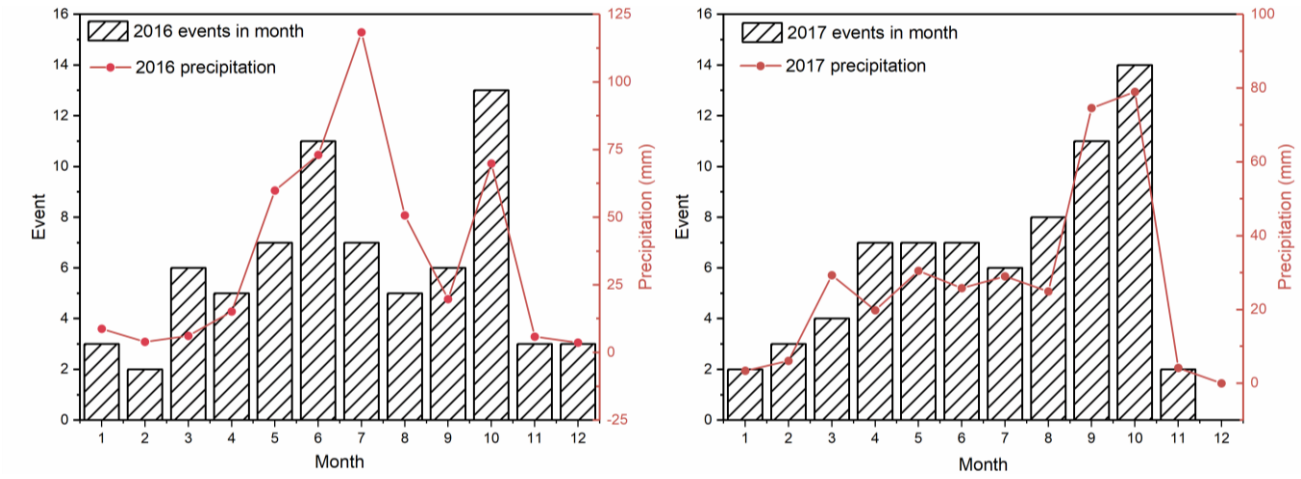

Figure S2. the distributions of the precipitation event and amount in the year

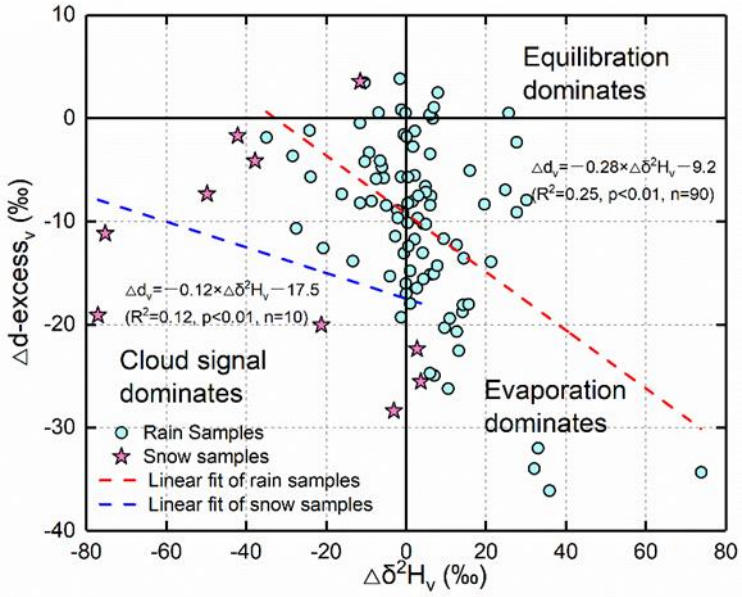

Figure S3. The projection of our data on Graf et al. (2019) suggested ΔdΔδ-diagram. The red dashed line corresponds to the linear fit of rain samples, and the blue dashed line represents to the linear fit of snow samples.

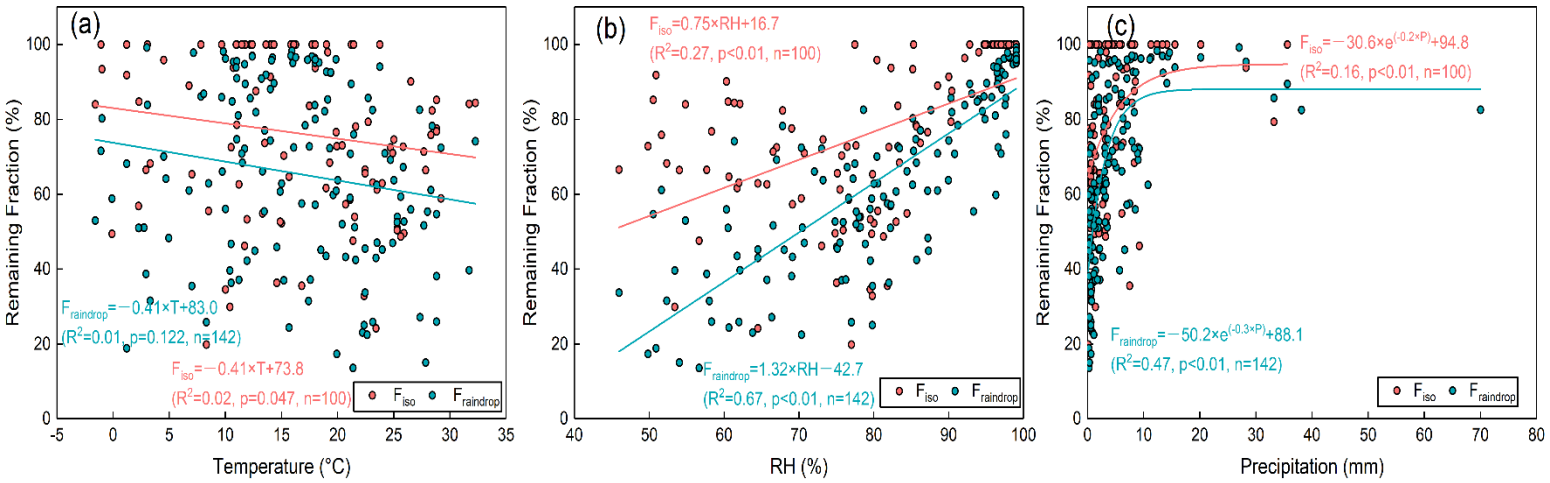

Figure S4 The correlations between the temperature and the remaining fraction calculated by isotopic method (light red dots) and mass conservation method (light blue dots) (a); the RH (b); and the precipitation amount (c).

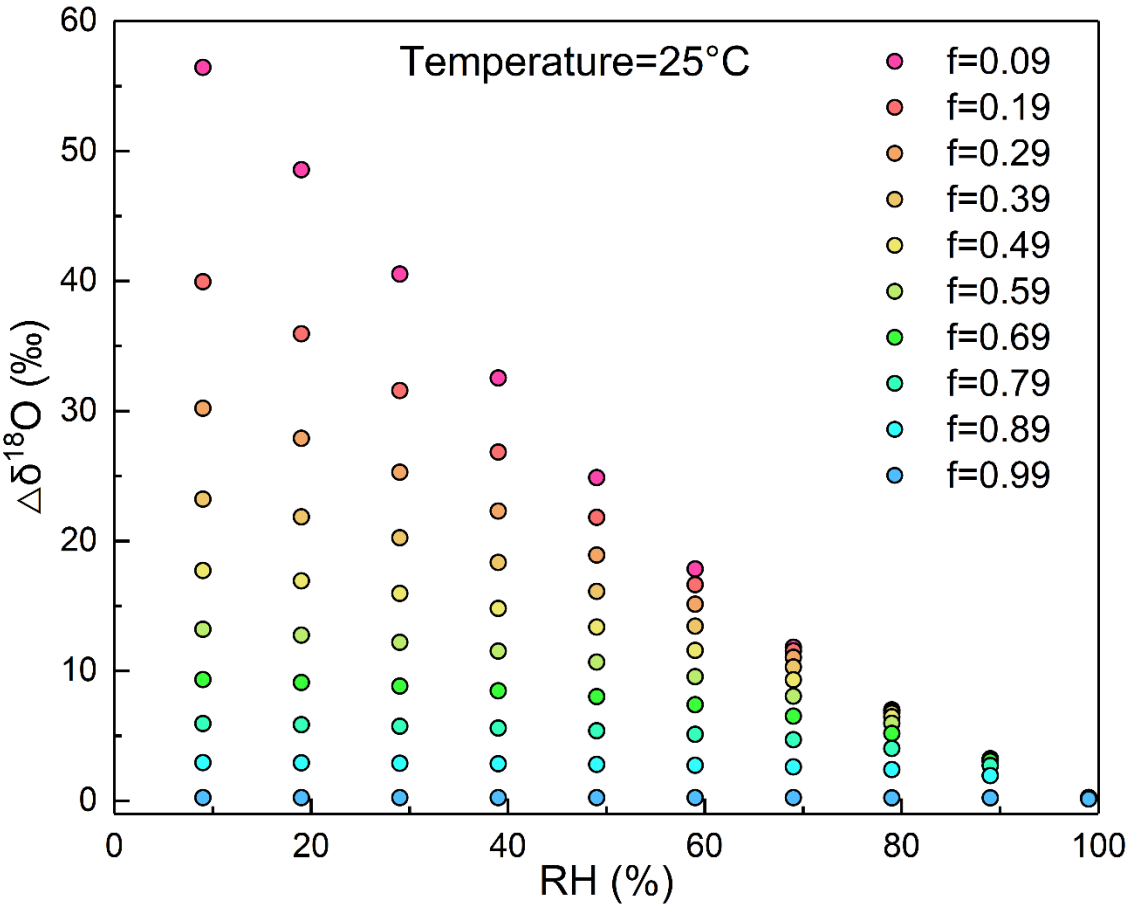

Figure S5 Sensitivity test of the variations between RH and $\Delta\delta^{18}O$ under different remaining fractions (f). We set the temperature at 25 °C indicating the equilibrium fractionation factor is calculated at 25 °C.

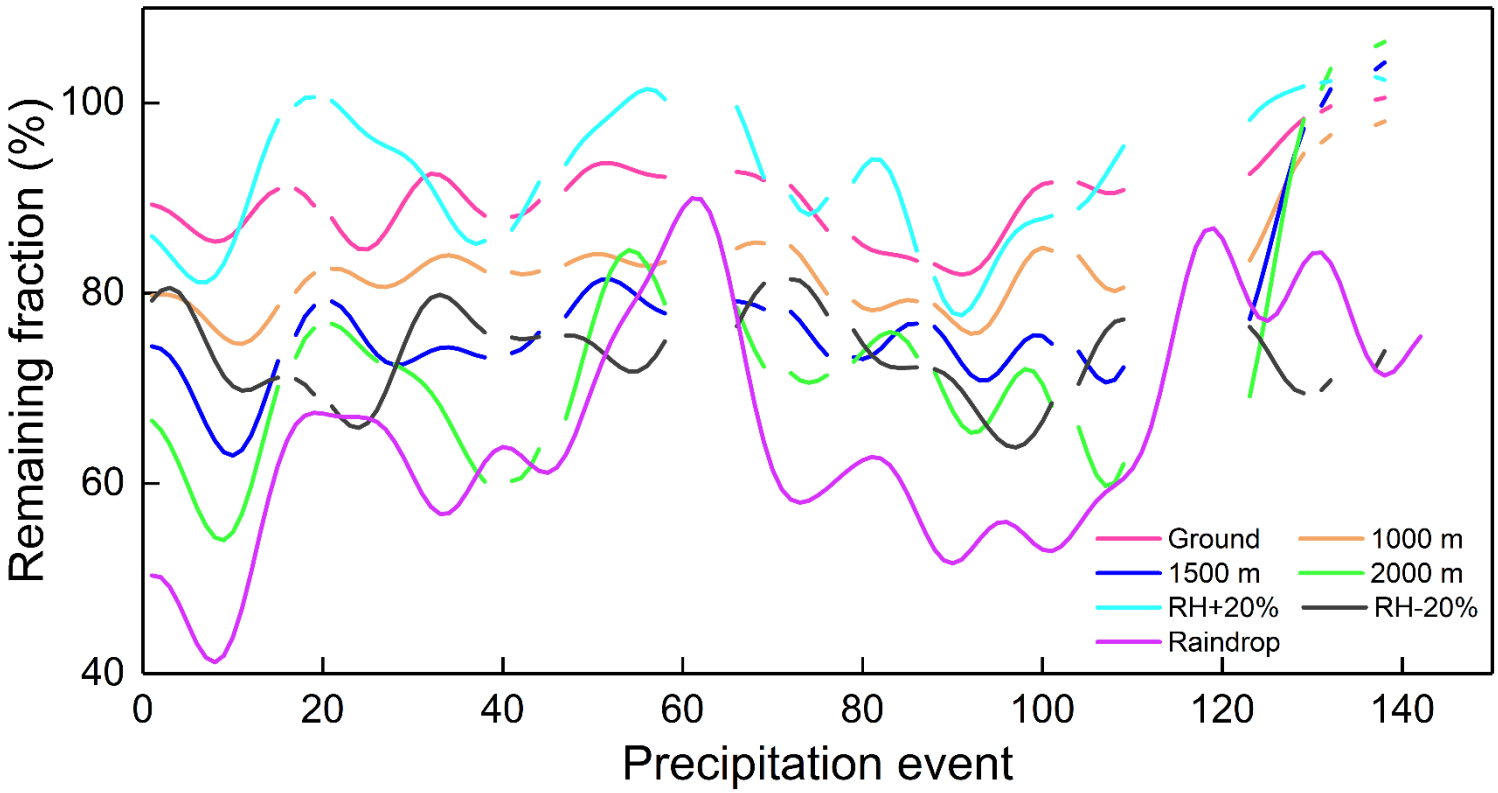

Figure S6 Sensitivity test of remaining fraction of evaporated raindrops under different cases. Ground represents the equilibrium fractionation factor is calculated based on the ground observed temperature, 1000m represents the equilibrium fractionation factor is calculated based on ambient temperature at 1000m, 1500m represents the equilibrium fractionation factor is calculated based on ambient temperature at 1500m, 2000m represents the equilibrium fractionation factor is calculated based on ambient temperature at 2000m, RH+20% represents the based on 1500m condition we increase the observed RH by 20%, RH-20% represents the based on 1500m condition we decrease the observed RH by 20%, and raindrop represents the remaining fraction is computed according to the mass conservation method. As the results with a large variation, we perform a 5-point smoothing on the data based on the Fast Fourier Transform method.

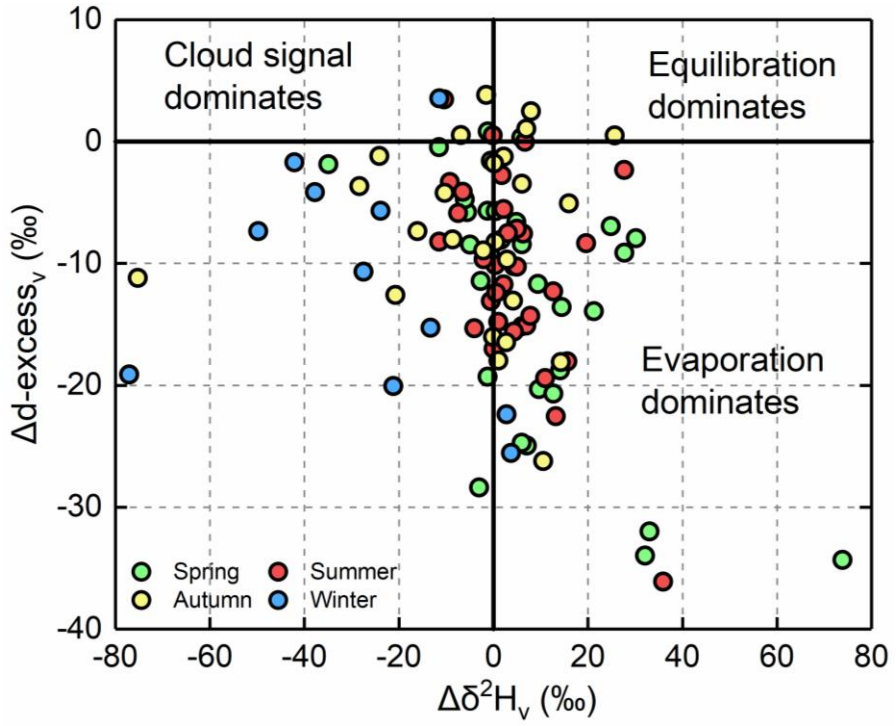

Figure S7 The projection of our data on ∆d∆δ-diagram and separated by seasons.

Table S1. Summary of event-based meteorological, precipitation, and water vapor data used in this study

Date	Type	T	RH	P	Duration	$\delta^{18}O_p$	$\delta^{2}H_p$	d-excess$_p$	$\delta^{18}O_v$	$\delta^{2}H_v$	d-excess$_v$
		°C	%	mm	h	‰	‰	‰	‰	‰	‰
2016-01-12	Snow	-0.1	80	1.3	13.0	-3.3	-32.4	-6.0	-22.5	-163.4	16.3
2016-01-22	Snow	-1.6	55	1.2	4.0	-15.8	-106.0	20.4	-29.5	-214.9	21.2
2016-01-31	Snow	-1.0	85	6.3	12.0	-8.7	-41.8	27.8	-19.2	-127.5	26.4
2016-02-12	Snow	4.5	80	3.8	9.0	-4.6	-20.1	16.7	-14.0	-90.4	21.4
2016-02-21	Snow	1.2	51	0.2	6.0	-10.1	-61.4	19.4	-21.1	-144.7	23.8
2016-03-04	Rain	10.4	53	1.4	4.0	8.8	61.2	-9.2	-16.1	-114.9	14.2
2016-03-09	Snow	3.3	52	0.6	7.0	0.6	18.3	13.5	-17.5	-105.8	34.4
2016-03-22	Rain	11.2	66	2.2	15.0	2.8	24.7	2.3	-12.0	-87.4	8.2
2016-03-23	Rain	10.5	82	0.8	21.0	-0.7	13.4	19.0	-11.7	-82.9	11.0
2016-03-24	Rain	8.3	77	0.1	5.0	1.2	8.6	-1.0	-14.1	-100.8	11.9
2016-03-25	Rain	8.5	81	1.1	4.0	-5.1	-32.5	8.3	-17.6	-127.3	13.7
2016-04-02	Rain	19.9	50	0.6	8.0	0.3	7.6	5.2	-12.7	-87.7	13.7
2016-04-05	Rain	11.0	86	3.6	7.0	0.8	12.2	5.8	-12.7	-83.3	18.4
2016-04-06	Rain	12.2	98	2.0	19.0	0.5	14.5	10.5	-13.3	-87.0	19.1
2016-04-15	Rain	12.7	90	8.3	12.0	-6.0	-35.5	12.5	-17.0	-120.1	16.1
2016-04-19	Rain	17.4	58	0.7	3.0	3.4	18.9	-8.5			
2016-05-07	Rain	13.3	84	6.1	19.0	1.6	24.0	11.5	-10.6	-72.6	12.4
2016-05-13	Rain	11.7	73	9.2	6.0	1.3	12.0	1.8	-14.0	-98.0	14.0
2016-05-14	Rain	10.7	97	28.2	19.0	-8.9	-55.5	15.6	-15.9	-111.2	16.3
2016-05-23	Rain	18.5	68	6.6	16.0	-2.3	-5.2	13.5			
2016-05-26	Rain	15.2	76	1.4	12.0	-4.2	-30.6	2.6	-16.0	-115.7	12.7
2016-05-27	Rain	14.0	97	4.9	21.0	-4.9	-26.6	12.2	-17.2	-121.0	16.7
2016-05-31	Rain	21.5	78	3.5	9.0	6.3	33.3	-17.4	-12.2	-85.1	12.6
2016-06-01	Rain	19.0	97	8.1	11.0	-0.1	3.5	4.1	-13.3	-90.0	16.2
2016-06-02	Rain	16.0	99	7.6	21.0	-3.0	-16.9	7.0	-15.0	-105.4	14.6
2016-06-03	Rain	20.4	78	0.4	1.0	-4.6	-23.1	13.4	-15.4	-107.6	15.6
2016-06-04	Rain	23.4	65	0.5	1.0	5.6	25.5	-19.3	-13.5	-94.0	13.7
2016-06-07	Rain	24.7	67	9.0	2.0	-4.8	-32.6	6.1	-16.5	-114.5	17.2
2016-06-11	Rain	26.5	60	8.5	4.0	-5.2	-23.6	17.7	-13.1	-89.7	15.5
2016-06-12	Rain	24.9	71	0.5	1.0	-2.6	-10.3	10.4	-14.2	-95.7	17.7
2016-06-23	Rain	22.7	90	33.2	15.0	-6.3	-37.3	13.3	-15.6	-107.3	17.3
2016-06-24	Rain	25.0	73	3.2	2.0	-5.5	-32.0	12.0	-16.3	-111.5	18.7
2016-06-25	Rain	25.3	78	0.5	1.0	-2.1	-17.9	-1.3	-14.4	-100.4	14.9
2016-06-30	Rain	28.8	51	1.6	0.5	-5.1	-36.2	4.3	-14.2	-98.1	15.3
2016-07-02	Rain	28.3	52	1.2	0.2	-2.2	-19.1	-1.5	-13.7	-95.2	14.6
2016-07-11	Rain	28.8	69	0.2	0.5	-8.5	-56.5	11.8	-18.8	-135.0	15.3
2016-07-12	Rain	28.8	58	0.5	2.0	-7.1	-50.3	6.4	-18.1	-127.5	17.1
2016-07-14	Rain	21.2	93	35.6	16.0	-8.6	-66.6	2.0	-20.3	-144.3	18.0
2016-07-19	Rain	24.2	89	8.9	14.0	-5.3	-51.3	-9.2			
2016-07-25	Rain	27.3	79	70.0	8.0	-9.3	-65.8	8.3			
2016-07-26	Rain	25.9	75	2.0	3.0	-6.2	-46.3	3.5	-19.4	-141.2	14.1
2016-08-02	Rain	29.2	70	3.1	0.5	-6.5	-42.8	9.0	-19.7	-143.0	14.5
2016-08-10	Rain	28.4	68	2.9	0.2	-9.3	-67.1	7.4	-18.7	-138.3	11.2
2016-08-19	Rain	31.7	62	5.7	8.0	-6.1	-43.2	5.6	-15.1	-105.9	15.1
2016-08-25	Rain	23.1	88	38.1	17.0	-5.7	-34.2	11.4			
2016-08-26	Rain	22.2	64	0.9	10.0	4.7	11.3	-26.6			
2016-09-12	Rain	20.7	69	2.7	7.0	0.4	-5.3	-8.8	-13.9	-103.5	7.8
2016-09-13	Rain	21.1	77	0.7	1.0	-1.3	-9.6	1.0	-13.7	-96.9	12.4
2016-09-19	Rain	17.7	99	8.4	15.0	-7.5	-45.9	14.3	-17.2	-119.3	18.4
2016-09-20	Rain	18.0	99	3.8	16.0	-6.5	-42.0	9.8	-18.0	-126.1	18.2
2016-09-24	Rain	21.6	86	0.9	8.0	-3.5	-35.0	-7.3	-16.0	-116.6	11.6
2016-09-26	Rain	19.1	94	3.3	4.0	-6.3	-42.8	7.4	-15.6	-109.2	15.3
2016-10-06	Rain	14.2	98	11.3	9.0	-4.3	-20.7	13.7	-16.0	-108.4	19.7
2016-10-08	Rain	16.8	82	7.5	26.0	-4.8	-23.6	14.4	-17.0	-113.1	22.6
2016-10-09	Rain	13.5	86	6.3	7.0	-6.5	-43.2	9.1	-16.4	-111.0	20.1
2016-10-12	Rain	14.1	99	0.3	1.0	-3.3	-20.9	5.9	-16.2	-110.8	18.6
2016-10-14	Rain	15.0	80	3.3	7.0	-3.2	-33.7	-8.4	-18.6	-132.0	16.7
2016-10-15	Rain	13.6	98	1.5	4.0	-8.0	-54.6	9.1	-18.8	-133.3	17.1
2016-10-21	Rain	17.1	91	7.1	12.0	-9.1	-65.3	7.6			
2016-10-22	Rain	13.2	97	7.0	13.0	-6.6	-32.3	20.7			
2016-10-23	Rain	11.7	99	2.7	11.0	-9.0	-50.8	21.0			
2016-10-24	Rain	10.0	97	9.5	8.0	-14.3	-98.3	15.7			
2016-10-25	Rain	9.8	99	2.3	3.0	-13.0	-91.3	13.1			
2016-10-26	Rain	11.0	99	4.2	21.0	-12.1	-81.8	15.4			
2016-10-27	Rain	10.6	94	6.9	17.0	-11.1	-73.6	15.6			
2016-11-06	Rain	11.0	97	0.8	2.0	-6.7	-35.5	18.2	-16.9	-120.8	14.7
2016-11-07	Rain	10.0	80	0.7	3.0	-6.1	-27.1	22.0	-20.0	-137.3	22.8
2016-11-22	Snow	-1.1	85	4.4	21.0	-12.3	-76.7	21.9	-19.8	-124.8	33.9
2016-12-03	Rain	7.0	80	0.5	11.0	-5.8	-34.0	12.2	-20.1	-134.5	26.5
2016-12-21	Rain	4.7	77	2.1	7.0	-3.8	-13.4	17.3			
2016-12-25	Snow	2.7	70	1.1	7.0	-3.4	-17.7	9.3			

Appendix of Table S1

Date	Type	T	RH	P	Duration	$\delta^{18}O_p$	$\delta^{2}H_p$	d-excess$_p$	$\delta^{18}O_v$	$\delta^{2}H_v$	d-excess$_v$
		°C	%	mm	h	‰	‰	‰	‰	‰	‰
2017-01-06	Rain	3.0	98	1.5	29.0	-7.0	-40.0	15.7	-19.6	-136.3	20.5
2017-01-07	Rain	2.3	61	1.9	7.0	-9.6	-64.4	12.1	-22.5	-155.5	24.3
2017-02-07	Snow	2.3	82	1.3	18.0	-2.5	-10.8	9.3	-17.4	-115.0	24.5
2017-02-08	Snow	2.9	58	1.1	8.0	-3.8	-24.8	5.6	-21.9	-149.8	25.2
2017-02-21	Snow	1.2	77	3.7	12.0	-9.0	-68.2	3.7	-16.9	-111.1	24.2
2017-03-13	Rain	3.0	99	27.0	10.0	-9.9	-60.6	18.4			
2017-03-15	Rain	4.9	87	0.5	9.0	-2.3	-9.8	8.7			
2017-03-23	Rain	6.8	89	0.6	5.0	0.1	17.0	16.3	-14.8	-102.0	16.7
2017-03-30	Rain	11.9	80	1.3	12.0	-2.7	-4.7	16.7	-18.6	-128.9	19.7
2017-04-03	Rain	14.6	75	0.9	5.0	1.8	5.9	-8.3	-13.1	-93.1	11.7
2017-04-08	Rain	14.9	83	1.7	6.0	-2.1	-1.6	15.0	-14.7	-98.5	19.3
2017-04-09	Rain	9.7	96	3.8	20.0	-4.2	-14.3	19.5	-16.0	-105.3	22.6
2017-04-10	Rain	7.8	95	6.0	21.0	-8.3	-49.4	17.1	-19.6	-138.1	19.0
2017-04-16	Rain	14.0	90	5.1	16.0	-2.6	-0.7	20.5	-14.3	-93.1	21.1
2017-04-19	Rain	15.7	61	0.6	5.0	0.8	-0.5	-7.1	-13.8	-96.5	13.9
2017-04-25	Rain	17.6	76	1.7	17.0	2.2	26.9	9.1			
2017-05-03	Rain	14.3	95	14.1	16.0	-5.5	-23.7	20.4	-17.0	-119.0	17.2
2017-05-14	Rain	21.4	57	0.2	6.0	8.3	55.4	-11.3	-10.1	-66.0	14.9
2017-05-15	Rain	17.5	83	6.0	6.0	-5.5	-30.2	13.6	-14.6	-104.1	13.1
2017-05-16	Rain	22.4	46	0.6	1.0	-3.1	-23.1	2.0	-17.8	-131.5	10.7
2017-05-22	Rain	19.3	83	8.3	8.0	-3.3	-9.3	17.3	-17.6	-119.4	21.8
2017-05-23	Rain	19.0	62	0.6	1.0	-3.3	-20.1	6.2	-18.1	-126.0	18.8
2017-05-29	Rain	23.1	62	0.6	4.0	4.1	33.3	0.3	-10.1	-63.9	17.2
2017-06-03	Rain	24.0	65	2.0	3.0	3.3	28.7	2.0	-10.5	-65.6	18.3
2017-06-04	Rain	15.9	99	12.4	8.0	-0.2	10.9	12.1	-12.7	-82.0	19.3
2017-06-05	Rain	15.8	99	7.9	16.0	-5.6	-31.4	13.7	-17.6	-121.5	19.3
2017-06-08	Rain	22.3	80	0.6	13.0	-2.6	-12.0	9.0	-15.4	-101.5	22.1
2017-06-09	Rain	21.4	98	0.5	8.0	0.2	0.4	-1.5	-14.5	-96.5	19.2
2017-06-10	Rain	22.4	75	2.2	6.0	-3.9	-19.1	12.4	-15.9	-105.1	21.9
2017-06-29	Rain	27.8	54	0.3	4.0	0.2	-1.9	-3.7	-13.6	-94.5	14.6
2017-07-05	Rain	27.3	66	0.3	2.0	-3.8	-41.3	-10.6			
2017-07-06	Rain	23.5	85	10.8	20.0	-9.2	-66.9	6.7			
2017-07-16	Rain	27.7	67	1.1	1.0	-6.6	-54.2	-1.6	-18.3	-127.3	19.1
2017-07-27	Rain	32.3	61	7.9	0.5	-10.5	-74.3	10.0	-19.4	-135.3	19.6
2017-07-28	Rain	23.7	96	5.7	2.0	-8.8	-67.3	3.0	-20.1	-139.0	21.8
2017-07-30	Rain	25.3	76	3.1	6.0	-7.5	-54.2	5.6	-20.4	-142.2	20.9
2017-08-13	Rain	25.8	76	5.1	3.0	-7.2	-48.5	9.2	-17.9	-121.7	21.3
2017-08-14	Rain	25.6	81	3.2	5.0	-7.4	-52.5	6.9	-18.8	-128.2	21.9
2017-08-21	Rain	28.0	78	0.8	1.0	-6.1	-46.0	2.7			
2017-08-25	Rain	22.6	70	1.1	17.0	1.0	2.3	-6.0			
2017-08-26	Rain	19.6	96	0.2	5.0	-2.0	-5.8	10.2			
2017-08-28	Rain	20.0	90	2.1	9.0	-10.9	-75.2	11.6			
2017-08-29	Rain	17.3	99	7.0	24.0	-10.7	-72.1	13.4			
2017-08-30	Rain	16.0	99	5.4	25.0	-11.4	-76.1	15.1			
2017-09-02	Rain	21.1	91	3.1	10.0	-13.9	-103.8	7.2			
2017-09-03	Rain	18.8	95	2.1	5.0	-12.9	-95.2	7.7			
2017-09-04	Rain	18.3	99	1.3	5.0	-11.2	-82.9	6.9			
2017-09-05	Rain	18.0	99	4.8	16.0	-15.7	-115.0	10.3			
2017-09-09	Rain	19.8	99	11.1	27.0	-12.7	-90.5	11.0			
2017-09-16	Rain	19.4	96	13.4	11.0	-5.9	-34.8	12.7			
2017-09-16	Rain	19.4	96	8.6	8.0	-6.1	-35.0	13.9			
2017-09-19	Rain	23.5	75	0.3	1.0	-2.8	-25.3	-3.2	-15.2	-107.4	14.0
2017-09-25	Rain	19.9	87	2.9	11.0	-9.1	-64.9	7.5	-20.5	-150.7	13.5
2017-09-26	Rain	18.0	82	7.0	24.0	-12.7	-90.1	11.6	-20.0	-141.2	18.8
2017-09-27	Rain	16.3	98	20.2	16.0	-9.8	-59.7	18.8	-20.8	-146.0	20.6
2017-10-01	Rain	18.0	95	3.2	12.0	-6.7	-41.2	12.2	-17.3	-124.4	13.8
2017-10-02	Rain	18.0	92	1.9	2.0	-7.5	-47.2	12.7	-18.2	-130.7	14.9
2017-10-03	Rain	12.4	98	13.3	9.0	-9.3	-53.0	21.6	-23.4	-167.7	19.9
2017-10-04	Rain	11.0	96	15.6	16.0	-18.2	-131.7	14.2	-28.6	-213.3	15.4
2017-10-08	Rain	16.1	97	0.6	10.0	-11.3	-79.4	11.3	-22.6	-168.9	12.2
2017-10-09	Rain	12.6	87	0.3	5.0	-9.3	-62.4	12.4			
2017-10-10	Rain	8.1	93	6.0	12.0	-13.3	-91.0	15.0			
2017-10-11	Rain	7.1	98	14.6	7.0	-17.0	-119.8	15.9			
2017-10-12	Rain	11.5	86	4.8	13.0	-17.6	-127.5	13.2			
2017-10-15	Rain	11.8	97	3.7	12.0	-13.9	-99.1	11.9	-22.0	-160.3	16.0
2017-10-16	Rain	11.5	97	0.3	12.0	-10.9	-69.9	17.5	-22.7	-166.3	15.0
2017-10-25	Rain	13.5	93	0.3	5.0	-3.9	-33.9	-2.8			
2017-10-30	Rain	10.5	79	0.3	2.0	-2.4	-18.3	0.6			
2017-11-01	Rain	11.1	96	1.2	10.0	-7.1	-37.6	19.3			
2017-11-10	Rain	9.7	72	3.0	4.0	-5.8	-25.5	21.2			

References

Araguás-Araguás, L., Froehlich, K. and Rozanski, K.: Deuterium and oxygen-18 isotope composition of precipitation and atmospheric moisture, Hydrol. Process., 14(8), 1341–1355, doi:10.1002/1099-1085(20000615)14:8<1341::AID-HYP983>3.3.CO;2-Q, 2000.

Best, A. C.: Empirical formulae for the terminal velocity of water drops falling through the atmosphere, Q. J. R. Meteorol. Soc., 76(329), 302–311, doi:10.1002/qj.49707632905, 1950a.

Best, A. C.: The size distribution of raindrops, Q. J. R. Meteorol. Soc., 76(327), 16–36, doi:10.1002/qj.49707632704, 1950b.

Deshpande, R. D., Maurya, A. S., Kumar, B., Sarkar, A. and Gupta, S. K.: Rain-vapor interaction and vapor source identification using stable isotopes from semiarid western India, J. Geophys. Res. Atmos., 115(23), 1–11, doi:10.1029/2010JD014458, 2010.

Ellehoj, M. D., Steen-Larsen, H. C., Johnsen, S. J. and Madsen, M. B.: Ice-vapor equilibrium fractionation factor of hydrogen and oxygen isotopes: experimental investigations and implications for stable water isotope studies, Rapid Commun. Mass Spectrom. Rcm, 27(19), 2149–2158, 2013.

Horita, J. and Wesolowski, D. J.: Liquid-vapor fractionation of oxygen and hydrogen isotopes of water from the freezing to the critical temperature, Geochim. Cosmochim. Acta, 58(16), 3425–3437, 1994.

Kinzer, G. D. and Gunn, R.: THE EVAPORATION, TEMPERATURE AND THERMAL RELAXATION-TIME OF FREELY FALLING WATERDROPS, J. Meteorol., 8(2), 71–83, doi:10.1175/1520-0469(1951)008<0071:TETATR>2.0.CO;2, 1951.

Kong, Y., Pang, Z. and Froehlich, K.: Quantifying recycled moisture fraction in precipitation of an arid region using deuterium excess . Tellus Series B Chem Phys Meteorol Quantifying recycled moisture fraction in precipitation of an arid region using deuterium excess, Tellus B, 65(August 2015), 1–8, doi:10.3402/tellusb.v65i0.19251, 2013.

Li, Z., Qi, F., Wang, Q. J., Kong, Y., Cheng, A., Song, Y., Li, Y., Li, J. and Guo, X.: Contributions of local terrestrial evaporation and transpiration to precipitation using δ 18 O and D-excess as a proxy in Shiyang inland river basin in China, Glob. Planet. Chang., 146, 140–151, 2016.

Parameswaran, K. and Murthy, B. V. K.: Altitude Profiles of Tropospheric Water Vapor at Low Latitudes, J. Appl. Meteorol., 29(8), 665–679, doi:10.1175/1520-0450(1990)029<0665:APOTWV>2.0.CO;2, 1990.

Stewart, M. K.: Stable isotope fractionation due to evaporation and isotopic exchange of falling waterdrops: Applications to atmospheric processes and evaporation of lakes, J. Geophys. Res., 80(9), 1133–1146, doi:10.1029/JC080i009p01133, 1975.

Sun, C., Chen, W., Chen, Y. and Cai, Z.: Stable isotopes of atmospheric precipitation and its environmental drivers in the Eastern Chinese Loess Plateau , China, J. Hydrol., 581(November 2019), 124404, doi:10.1016/j.jhydrol.2019.124404, 2020.

Wang, S., Zhang, M., Che, Y., Zhu, X. and Liu, X.: Influence of Below-Cloud Evaporation on Deuterium Excess in Precipitation of Arid Central Asia and Its Meteorological Controls, J. Hydrometeorol., 17(7), 1973–1984, doi:10.1175/JHM-D-15-0203.1, 2016.

Zhao, L., Liu, X., Wang, N., Kong, Y., Song, Y., He, Z., Liu, Q. and Wang, L.: Contribution of recycled moisture to local precipitation in the inland Heihe River Basin, Agric. For. Meteorol., 271(July 2018), 316–335, doi:10.1016/j.agrformet.2019.03.014, 2019.